

Investigating Miscibility of Polymers and Its Impact on the Morphology, Thermal, and Mechanical Properties of Polymer Blends

Zafarullah Khan Marwat¹ · Musa Kaleem Baloch¹

Received: 25 February 2014 / Accepted: 5 August 2015 / Published online: 28 August 2015
© Springer Science+Business Media New York 2015

Abstract The miscibility of polystyrene (PS)/poly(styrene-*co*-acrylonitrile) (PSAN) blend films, prepared by the solution casting technique using tetrahydrofuran as a common solvent, was characterized by scanning electron microscopy, differential scanning calorimetry (DSC), thermogravimetry, Fourier transform infrared (FTIR) spectroscopy, and tensile testing. Morphological observations revealed partial miscibility of the blend. FTIR measurements also ascertained partial miscibility of the blend as slight variations in the spectra for various blend compositions were observed. DSC studies also confirmed the semicompatible nature of the examined blend by displaying a single T_g for the composition, 25/75, and two T_g 's for compositions, 50/50 and 75/25. The enhancement in thermal stability and mechanical properties which were quite pronounced for the composition, 25/75, also favored partial miscibility of the blend. The partial miscibility of the PS/PSAN blend may be attributed to the intramolecular repulsive effect, characteristic of a homopolymer/copolymer blend system, and the Pi–Pi stacking of phenyl rings of the blend components due to some structural similarities.

Keywords Differential scanning calorimetry (DSC) · Fourier transform infrared (FTIR) · Miscibility · PS/PSAN blends · Morphology · Tensile testing · Thermogravimetric analysis (TGA)

1 Introduction

Polymer blending is an attractive and economical technique for producing new materials with improved properties by combining physically already existing polymers

✉ Zafarullah Khan Marwat
zkmarwat2002@gmail.com

¹ Department of Chemistry, Gomal University, Dera Ismail Khan, Pakistan

without having to synthesize totally new polymeric materials [1,2]. The main purpose of polymer blending is to achieve a synergistic effect in the resulting material. However, synergism in final properties depends on the miscibility of blend components at the molecular level as well as on the type of morphology, e.g., co-continuous structure. The coexistence of at least two continuous structures within the same volume is considered to be a co-continuous structure. Polymer blends having co-continuous morphologies generally combine the properties of both the constituents in a favorable way; this is why increased scientific and industrial interest has been observed in determining the miscibility and morphology of polymer blends [3–7]. However, most polymers are immiscible resulting in a heterogeneous system due to high interfacial tension and hence poor interfacial adhesion [8]. The characteristics of the component polymers, in immiscible blends, combine in such a way that the blend morphology is a real reflection of the component morphology [9]. Therefore, blend morphology is considered to be a good indicator of blend miscibility [10–13].

Interfacial adhesion between the phases plays a decisive role in controlling the extent of dispersion of a dispersed phase. That is why synergism in end properties is generally observed for a small-sized dispersed phase due to better compatibility of the blend components [10,12,14]. On the other hand, maximum synergy in the end properties has been observed for blends with miscible components at the molecular level, but there are cases of immiscible blends where synergism in some of the mechanical properties has been observed [15]. Thus, in such phase-separated systems, the overall thermomechanical behavior should depend mainly on two factors: a matching interfacial tension that can result in a phase having a size small enough to be classified as macroscopically homogeneous and having a strong interface adhesion in order to withstand stresses without any disturbance of the proven morphology [2]. Similarly, T_g values as a function of polymer blend composition may indicate the extent of the blend miscibility, partial miscibility, or total immiscibility [16]. A single composition-dependent T_g is considered as characteristic of complete miscibility, whereas two T_g 's that are composition dependent to a different extent and/or a single T_g composition dependent but in a narrow composition range may indicate partial miscibility of the binary blend. However, in the case of a totally immiscible blend system, the blend components may retain their original T_g values, independent of the blend composition [16,17].

A comprehensive understanding of thermal stability and degradation of polymers and their blends is not only necessary for their use in a number of consumer oriented applications but also to provide a knowledge about the miscibility of the blends. Thermogravimetric analysis is, therefore, extensively employed for probing the thermal stability of polymers and their blends [18,19]. Besides differential scanning calorimetry (DSC), Fourier transform infrared (FTIR) is also one of the most used analytical techniques used to reveal the extent of miscibility between polymers [20]. The shifting of a band corresponding to a determined functional group is interpreted as a direct consequence of intermolecular interactions due to the variations in electronic density of the chemical bonds involved in the interaction. If there are no appreciable changes in the FTIR spectra of the blends with respect to the co-addition of each component, it shows that the two polymers form completely immiscible blends [21]. However, a specific interaction existing in the case of miscible blends between the component

polymers results in a variation of IR spectra for the blend [22]. In this way FTIR can provide information about the miscibility of polymer blends by identifying segmental interactions [20]. We have, therefore, decided to employ these techniques to estimate the miscibility and its impact on thermal and mechanical properties of the polystyrene (PS)/poly(styrene-*co*-acrylonitrile) (PSAN) blend. The choice of PS and PSAN as component polymers is based on their useful mechanical and electrical properties and their applications in our daily life [23–27]. Moreover, a comprehensive literature survey also revealed that no significant work has been reported so far about the miscibility of solution-cast PS/PSAN/THF blends [5, 28, 29].

2 Experimental

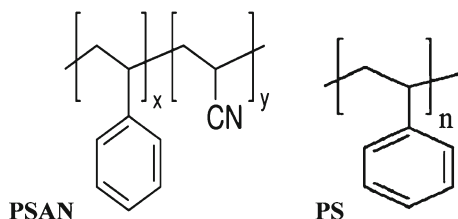
2.1 Materials

The two polymers used in this study, polystyrene and poly(styrene-*co*-acrylonitrile), were purchased from Aldrich, USA having mass-average molar masses, M_w , of $1.87 \times 10^5 \text{ g}\cdot\text{mol}^{-1}$ and $1.96 \times 10^5 \text{ g}\cdot\text{mol}^{-1}$, respectively, and their structures are displayed in Scheme 1. Poly(styrene-*co*-acrylonitrile) has 25 mass% of the AN content. The solvent, tetrahydrofuran (THF), procured from Fluka, Germany was of analytical grade and used as received.

2.2 Preparation of Blend Solutions and Films

PS/PSAN blends were prepared by a solution casting technique using THF as a common solvent. Solutions of PS, PSAN, and their blends were prepared in various mass ratios by dissolution of the required amount of component polymers in THF at a concentration of $5.0 \text{ g}\cdot\text{dL}^{-1}$ at ambient temperature. The resulting solutions were then allowed to stand for 48 h to ensure thorough mixing and better homogeneity. This mixture was subsequently cast onto a clean, dry, and smooth glass plate for film formation. The cast films were first dried under ambient conditions, at a low evaporation rate in order to avoid film cracking. The dried films were then peeled off from the glass plate and further dried in a vacuum oven at 60°C for 72 h to remove the residual solvent completely. The first numeral of the blend composition, throughout this paper, indicates the PS fraction.

Scheme 1 Representation of the structure of polymers used



3 Characterization Techniques

3.1 Scanning Electron Microscopy

A scanning electron microscope (SEM) LEO 440i was used to examine the phase structure of the PS/PSAN blends. Samples were fractured immediately after cooling in liquid nitrogen. The fractured surfaces of the dried samples were then sputter-coated with a thin layer of gold for enhancement of conductivity before scanning electron microscopy (SEM) analysis.

3.2 Fourier Transform Infrared Spectroscopy

FTIR measurements were carried out using an FTIR spectrometer, Tensor-27, supplied by Bruker, Germany in order to find out the interactions between PS and PSAN in the blend. The spectra of samples were recorded and stored in the spectral range of 4000 cm^{-1} to 500 cm^{-1} , with 35 scans at a resolution of 2 cm^{-1} .

3.3 Differential Scanning Calorimetry

A differential scanning calorimeter, Diamond, Perkin-Elmer, USA was employed to record differential scanning calorimetry curves of PS, PSAN, and their blends of different compositions. The sample was heated from $30\text{ }^{\circ}\text{C}$ to $200\text{ }^{\circ}\text{C}$ at a heating rate of $15\text{ }^{\circ}\text{C}\cdot\text{min}^{-1}$, under an atmosphere of nitrogen, and at a flow rate of $50\text{ mL}\cdot\text{min}^{-1}$. The DSC instrument was calibrated using pure indium metal. Samples of 5 mg to 8 mg were sliced and then compressed into aluminum pans used for testing purposes. One minute holding time was allowed at $30\text{ }^{\circ}\text{C}$ in each scan for isothermal scanning of the blend films. All the results were obtained from the second scan to eliminate thermal history effects.

3.4 Thermogravimetric and Differential Thermal Analysis

A thermal stability study of neat polymers and their blend was performed using thermogravimetry (TG)/DTA Diamond, Perkin-Elmer, USA. For the purpose, the samples weighing 5 mg to 8 mg were heated in aluminum pans from $50\text{ }^{\circ}\text{C}$ to $550\text{ }^{\circ}\text{C}$ at a heat flow rate of $15\text{ }^{\circ}\text{C}\cdot\text{min}^{-1}$ under a nitrogen gas atmosphere with a flow rate of $100\text{ mL}\cdot\text{min}^{-1}$.

3.5 Tensile Testing

Tensile tests were conducted on a Testometric materials testing machine, Rochdale, UK equipped with computer-controlled MTS Test Works software for data acquisition and analysis at ambient temperature. The film specimens with uniform dimensions of $36\text{ mm} \times 12\text{ mm}$ were cut by a stainless-steel razor blade, and the dimensions were measured using a Vernier caliper. The thickness of the films varied from 0.2 mm

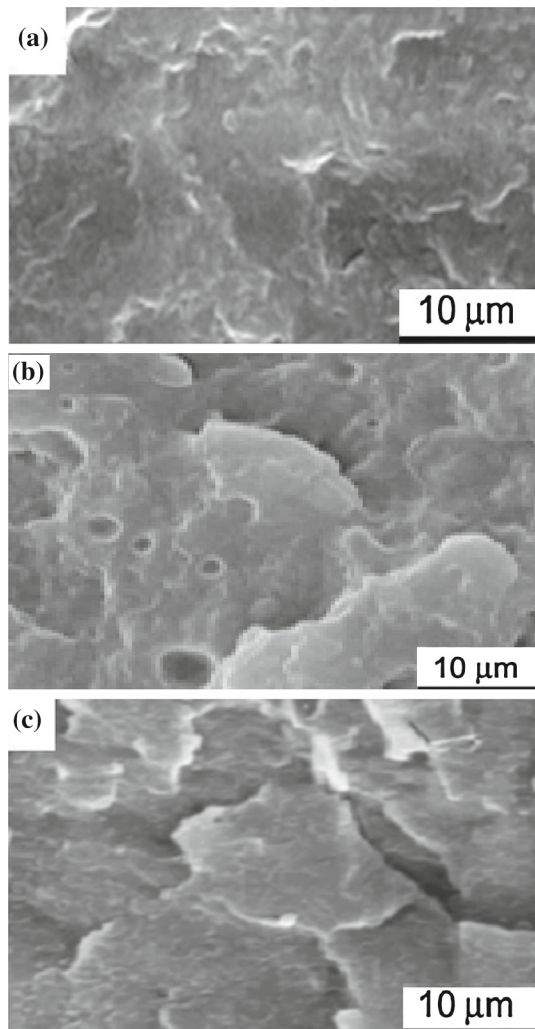
to 0.6 mm as measured with the help of a screw gage. The crosshead speed was maintained at $100 \text{ mm} \cdot \text{min}^{-1}$. Six samples for each composition were tested, and the average results are reported.

4 Results and Discussion

4.1 Morphological Analysis

The morphology has a strong impact on the properties of polymer blends [28–30]. The SEM images for different PS/PSAN blend (25/75, 50/50 and 75/25) compositions are displayed in Fig. 1a–c. The PS/PSAN blend (25/75 and 75/25) compositions (Fig. 1a,

Fig. 1 SEM images of PS/PSAN blend having PS/PSAN ratios as (a) 25/75, (b) 50/50, and (c) 75/25. The scale is given as insertion in each figure



c) clearly show that the PS and PSAN domains are dispersed on a fine scale in the PSAN and PS continuous phases, respectively. It can, thus, be concluded from Fig. 1a, c that the interfacial adhesion between the two phases at the given compositions is rather good, thereby, confirming the presence of some favorable interactions [33–35]. However, the composition, 50/50, having phase-separated rough morphology (Fig. 1b), indicates phase separation due to weak interactions between the two phases [36]. The morphological observations revealed partial miscibility of the blend.

4.2 FTIR Analysis

FTIR spectra of pure PS, PSAN, and their blends (0/100, 25/75, 50/50, 75/25, and 100/0) are depicted in Fig. 2a–e. It has been reported that the miscibility of PPO (poly(2,6-dimethyl-1,4-phenylene oxide))/PS blends could be accounted for by Pi–Pi stacking between the phenyl rings of the PPO and PS [37]. Thus, we also investigated the peaks of phenyl rings of PS, PSAN, and their blends by FTIR spectra. The phenyl ring C–H out-of-plane (OOP) bending, C–H aromatic bending, C=C aromatic ring stretching, C≡N, and C–H aromatic stretching in PS, PSAN, and their blends are shown in Table 1. A detailed analysis of FTIR spectra of PS, PSAN, and their blends indicated a decrease in the transmittance peaks of the phenyl ring C–H out-of-plane (OOP) bending, C–H aromatic bending, and C=C aromatic ring stretching with an increase in the PS content of the blend. On the other hand, an increase in the wave number for the nitrile (C≡N) group in all the blend compositions other than pure PSAN was observed. The only appreciable variations in the transmittance were observed in the case of C–H aromatic stretching. These variations in the vibration frequencies with an increase in the PS content of the blend could be accounted for by Pi–Pi stacking between the phenyl rings of the PS and PSAN. The partial miscibility of the PS/PSAN blend is thus likely to be the result of Pi–Pi stacking between the phenyl rings of the PS and PSAN.

4.3 DSC Analysis

DSC scans of PS, PSAN, and their blend films were performed and displayed in Fig. 3. T_g 's obtained from the mid-point of the slope of DSC curves [38] are listed in Table 2. PS and PSAN films showed a single T_g at 92 °C and 124 °C, respectively. The blend composition, 25/75, showed a single composition-dependent T_g whereas compositions, 50/50 and 75/25, showed two T_g 's (Fig. 4), indicating partial miscibility of the blend [16].

4.4 TG Analysis

TG curves indicating mass% as a function of temperature for PS, PSAN, and their blends are shown in Fig. 5. All the TG curves indicated single-stage degradation. Minor mass losses for neat polymers and their blends observed from 30 °C to 100 °C were assigned to solvent evaporation. The major mass losses that happened beyond

Fig. 2 FTIR Spectra of films of PS, PSAN, and PS/PSAN blends having ratios (a) 0/100, (b) 25/75, (c) 50/50, (d) 75/25, and (e) 100/0. The films were prepared by dissolving the polymers in THF and drying at 60 °C

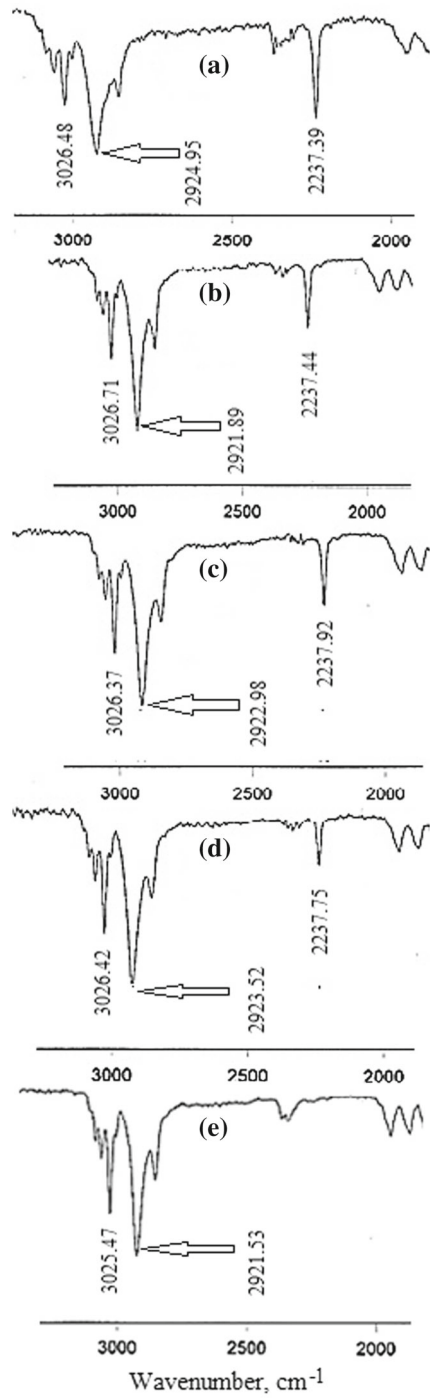
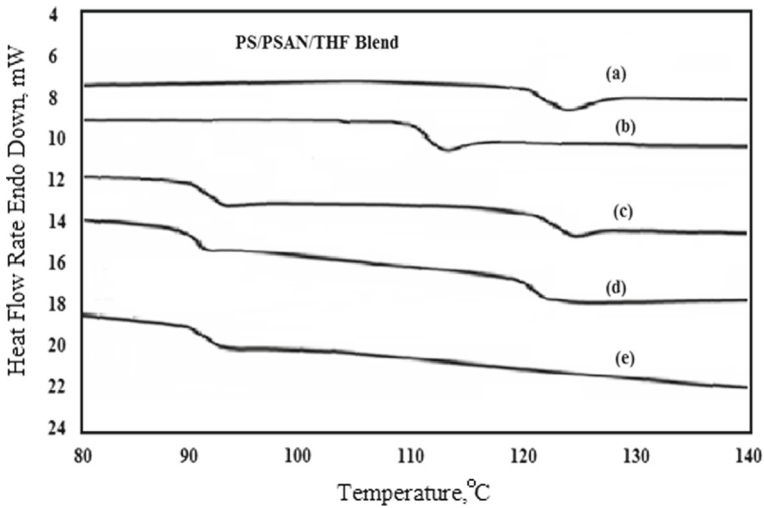


Table 1 FTIR results for PS, PSAN, and PS/PSAN/THF blends in wave numbers (cm^{-1})

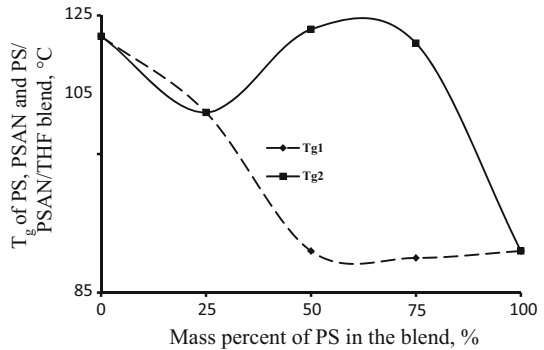
Solvent	PS:PSAN	Bonds				
		C–H OOP bending	C–H aromatic bending	C=C aromatic ring stretching	C≡N	C–H aromatic stretching
THF	0:100	1028.71	1452.68	1493.57	2237.39	2924.95 and 3026.48
	25:75	1028.36	1452.68	1493.29	2237.44	2921.89 and 3026.71
	50:50	1028.32	1452.56	1493.19	2237.92	2922.98 and 3026.37
	75:25	1028.15	1452.25	1493.13	2237.75	2923.52 and 3026.42
	100:0	1027.86	1451.84	1492.55	–	2921.53 and 3025.47

**Fig. 3** DSC curves of films of PS, PSAN, and PS/PSAN/THF blends having ratios (a) 0/100, (b) 25/75, (c) 50/50, (d) 75/25, and (e) 100/0**Table 2** T_g values of PS, PSAN, and their blends

PS/PSAN blend composition	T_{g1} ($^{\circ}\text{C}$)	T_{g2} ($^{\circ}\text{C}$)
0/100		122
25/75	111	
50/50	91	123
75/25	90	121
100/0	91	

350 $^{\circ}\text{C}$ were due to structural decomposition of the polymers and their blends [39]. The obtained data indicated that thermal degradation of PS was considerably slowed down by the incorporation of PSAN in the blends. The higher degradation temperatures for 25/75 and 75/25 blend composition as compared to 50/50 and neat polymers were attributed to some favorable interactions between blend components [33–35]. In order

Fig. 4 Plot of T_g as function of PS content in the PS/PSAN/THF blend



to further highlight the impact of blending on the thermal stability, the mass% was evaluated at different temperatures from 100 °C to 432 °C, and tabulated in Table 3. The comparison of the values of the mass% of PS, PSAN, and their blends also indicated that during the degradation process, for any fixed temperature, the thermal stability for pure polymers and various blend compositions was in the order, 25/75 > 75/25 > 0/100 > 100/0 > 50/50. Thermogravimetric results also favored partial miscibility of the blend under study.

4.5 Miscibility and Mechanical Properties of Polymer Blend

Depending on the extent of miscibility, ranging from complete miscibility to immiscibility, the mechanical properties of the polymer blends vary between those of the

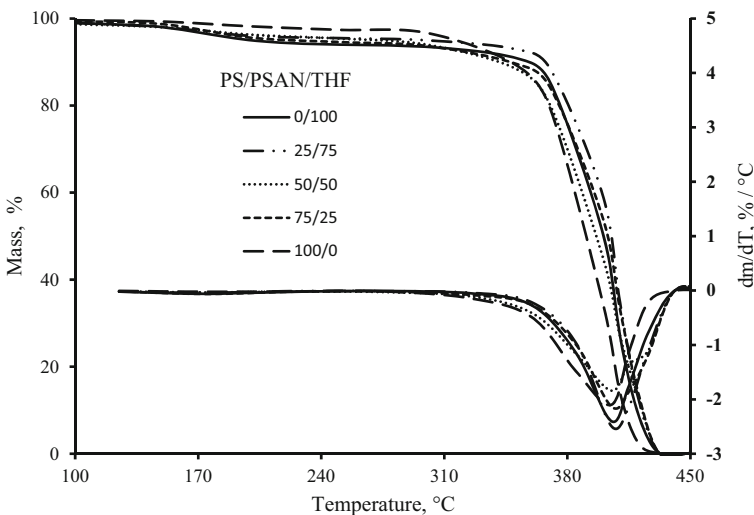
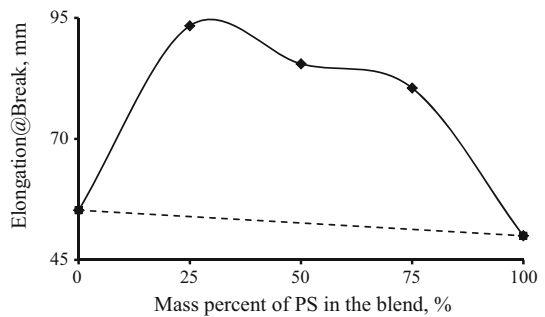


Fig. 5 TG and dTG curves of films of PS, PSAN, and their blends. The indicated number in the figure shows the ratio of PS to PSAN

Table 3 Thermal data obtained from TGA curves of PS, PSAN, and PS/PSAN/THF blends

Temp. (°C)	Mass% of PS, PSAN, and PS/PSAN/THF blends at various temperatures				
	0/100	25/75	50/50	75/25	100/0
100	99	99	98.7	99.4	99.6
150	98	98	98	98.7	99.3
200	95	96	96.3	95.6	98.2
250	94	95.5	95.4	94.6	97.4
300	93.5	95	94	93.7	96.7
350	91	93	88.6	89.7	89.5
370	85.5	88.6	80.3	84.3	79.6
400	51	59.6	45.4	54.4	35
410	27	34.7	27	33.1	14
420	9.5	13.3	13.5	14.5	2.7
432	0.2	0.28	0.24	0.3	0.1

Fig. 6 Elongation at breaking points of PS, PSAN, and their blends as a function of mass percent of PS

neat polymers [40]. A linear relationship between the mechanical properties and the blend composition indicates miscibility of the system. However, positive and negative deviations from the linear relationship indicate enhancement in miscibility and immiscibility between blend components, respectively [41].

Mechanical property measurements for neat polymers and their blends as a function of mass% of PS in the blend are shown in Figs. 6, 7, 8, 9, and 10, and their values are tabulated in Table 4. Keeping in view the fact that mechanical properties of the resulting blend depend mainly on the properties of its components, we connected the values from 0 mass% to 100 mass% for PS by a dotted line indicating a weighted average.

The elongation at the breaking points for different compositions showed positive deviations from simple additivity over the entire composition range, indicating better interfacial adhesion between the blend components and hence an enhancement in ductility (Fig. 6). Despite positive deviations, a steady decrease in the elongation at the breaking points for different PS/PSAN blend (25/75, 50/50, 75/25) compositions with an increase in mass% of PS in the blend was also observed which may be attributed

Fig. 7 Energy to break films of PS, PSAN, and their blends as a function of mass percent of PS

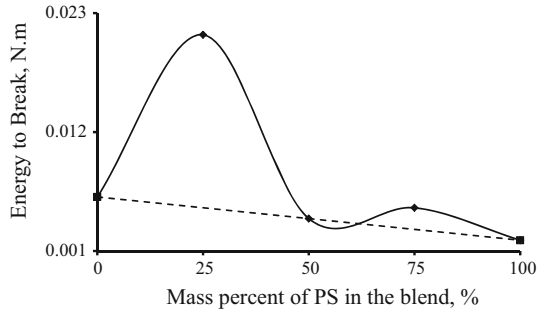


Fig. 8 Strain at breaking points of PS, PSAN, and their blends as a function of mass percent of PS

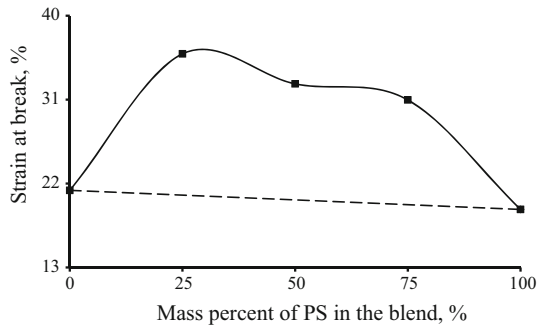


Fig. 9 Tensile strength of PS, PSAN, and their blends as a function of mass percent of PS

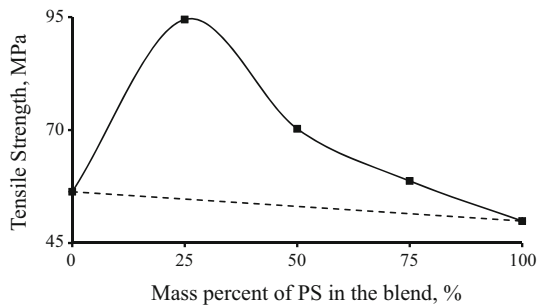


Fig. 10 Young's modulus of PS, PSAN, and their blends as a function of mass percent of PS

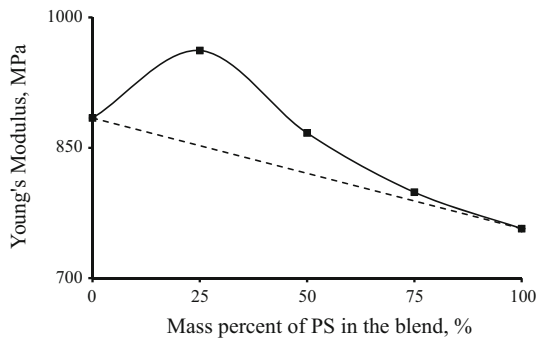


Table 4 Mechanical properties data

	PS (mass%)				
	0	25	50	75	100
Elongation @ breaking point (mm)	55	93	86	81	50
Energy to break (N·m)	0.006	0.021	0.004	0.005	0.002
Tensile strength (MPa)	56	94	70	59	50
Young's modulus (MPa)	884	962	867	799	757
Strain@ breaking point (%)	21	36	33	31	19

to a decrease in the interfacial adhesion between two phases with an increase in PS content. The plausible explanation for this is that by increasing the amount of PS in the blend, the styrene proportion contributed by PS increases but at the same time a decrease in the styrene proportion contributed by PSAN also occurs, which results in weakening of Van der Waals interactions between the two phases due to the fact that the homopolymer (PS) chains cannot be solubilized into the block domains of the same type (PSAN) provided that the molecular mass of the former is the same as or less than that of the latter [42]. Moreover, a decrease in the PSAN content in the blend is also responsible for deterioration of the elongation at the breaking points [43].

The energy to break the films also indicated positive deviations from the rule of mixtures for the blend (25/75 and 75/25) compositions. However, the composition, 50/50, neither showed a positive nor negative deviation but just lay on the dotted line (Fig. 7). The highest energy for a breaking value for the blend composition, 25/75, among various blend (50/50 and 75/25) compositions indicates rather good adhesion between the dispersed and matrix phases due to better phase dispersion which resulted in an improvement in the plastic nature of the said composition as compared with the other blend (50/50 and 75/25) compositions [42].

The strain at the breaking points showed almost the same behavior as that of the elongation at the breaking points. All the three blend compositions indicated positive deviations from simple additivity (Fig. 8). These results confirm the presence of some favorable interactions between the blend components that is strongest in composition, 25/75.

The tensile strength (TS) is an important characteristic of polymeric materials because it shows the limit of final stress for most applications. The TS values of all the blend compositions show positive deviations from the dotted line (Fig. 9). There is an increase in TS from 0/100 (pure PSAN) to the composition, 25/75. Beyond the composition, 25/75, a rapid fall in TS values occurs reaching finally a minimum value for 100/0 (pure PS). These results suggested a partial compatibility between PS and PSAN. Miscibility results from physical entanglements, some similarity in the chemical structure of PS and PSAN (styrene parts) [44], the intramolecular repulsive effect of the homopolymer copolymer system [33–35], in addition to the superior tensile strength of PSAN [43].

The Young's modulus of the blends also showed positive deviations from the rule of mixtures that decreased with an increase in the PS content of the blend (Fig. 10). The

Young's modulus was also affected by the blend composition. Efficient interfacial adhesion between the component polymers could account for the observed higher Young's modulus of the composition, 25/75, compared to the other two compositions (50/50 and 75/25). The Young's modulus versus mass % of PS showed almost the same trend as was observed in the case of the tensile strength (Fig. 10).

5 Conclusions

Microscopy, FTIR, DSC, TG/DTA, and tensile testing techniques were employed for investigation of PS/PSAN blend miscibility. Morphological studies revealed heterogeneity for all compositions of the blend with different domain sizes which was larger in composition 50/50 compared to the other compositions, 25/75 and 75/25. The smaller domain size of the latter blend compositions is attributed to the better dispersion of the minor phase into the major one, thus resulting in better adhesion between the dispersed phase and matrix. FTIR spectroscopy indicated the absence of any specific interactions in different blend compositions as no appreciable shifts in wave numbers were observed in them with respect to neat polymers. On the other hand, DSC results revealed partial miscibility of the blend by displaying a single T_g for the composition, 25/75, and two T_g 's for compositions, 50/50 and 75/25. TG measurements also showed high thermal stability for blend compositions, 25/75 and 75/25, and less thermal stability for the composition, 50/50, as compared with the neat polymers. Almost all the blend compositions showed synergism in mechanical properties as they were lying above the additivity line. A decrease in the synergistic behavior with an increase in PS content of the blend was also observed. The blend composition, 25/75, showed optimum thermal and mechanical results that may be attributed to better solubilization of a minor PS part into the major PSAN part due to structural similarity and an intramolecular repulsive effect, characteristic of a homopolymer/copolymer blend system. A good correlation among the morphology, spectroscopic, thermal, and tensile results was found. Thus, keeping in view the results obtained through different techniques, the PS/PSAN blend is classified as a partially miscible blend system.

Acknowledgments Financial assistance from the Higher Education Commission, Islamabad, Pakistan, via an Indigenous Ph.D. Fellowship and the grant of study leave for Ph.D. studies by the Higher Education Department, Khyber Pakhtoonkhwa, Peshawar, Pakistan to Zafarullah Khan Marwat is gratefully acknowledged.

References

1. D.R. Paul, C.B. Bucknall, *Polymer Blends: Formulations and Performance* (Wiley, New York, 2000)
2. L.A. Utracki, *Polymer Alloys and Blends: Thermodynamics and Rheology* (Oxford University Press, New York, 1989)
3. A.K. Kulshreshtha, B.P. Singh, Y.N. Sharma, *Eur. Polym. J.* **24**, 33 (1988)
4. O. Olabisi, L.M. Robeson, M.T. Shaw, *Polymer-Polymer Miscibility* (Academic Press, New York, 1979)
5. Z. Khan, M.K. Baloch, *Polym. Bull.* **70**, 2015 (2013)
6. Z. Khan, M.K. Baloch, *J. Macromol. Sci. Part B* **53**, 1027 (2014)
7. Z.K. Marwat, M.K. Baloch, *Chin. J. Polym. Sci.* **32**, 1442 (2014)

8. A. Boztug, H.B. Zengin, S. Basan, J. Mol. Struct. **697**, 61 (2004)
9. C.Z. Chuaia, K. Almdalc, J. Lyngaae-Jørgensenb, Polymer **44**, 481 (2003)
10. C. Sirisinha, S. Limcharoen, J. Thunyarittikorn, J. Appl. Polym. Sci. **82**, 1232 (2001)
11. C. Boisserie, R.H. Marchessault, J. Polym. Sci. **15**, 1211 (1977)
12. J. Clarke, B. Clarke, P.K. Freakley, Rubber Chem. Technol. **74**, 1 (2001)
13. G. Severe, J. White, J. Appl. Polym. Sci. **78**, 1521 (2000)
14. O. Chung, A.Y. Coran, Rubber Chem. Technol. **70**, 781 (1997)
15. J. Ramiro, J.I. Eguiazabal, J. Nazabal, Euro. Polym. J. **42**, 458 (2006)
16. Witold Brostow, Rachel Chiu, Ioannis M. Kalogeras, Aglaia Vassilikou-Dova, Mater. Lett. **62**, 3152 (2008)
17. R. Wunderlich, *Thermal Analysis* (Academic Press, New York, 1990)
18. P.S. Archondouli, J.K. Kallitsis, N.K. Kalfoglou, J. Appl. Polym. Sci. **88**, 612 (2003)
19. M.E. Brown, P.K. Gallagher, *Handbook of Thermal Analysis*, vol. 2 (Elsevier, Amsterdam, 2003), p. 112
20. X.F. Ma, J.G. Yu, N. Wang, J. Polym. Sci. Part B **44**, 94 (2006)
21. G.B. Zhang, J.M. Zhang, X.S. Zhou, D.Y. Shen, J. Appl. Polym. Sci. **88**, 973 (2003)
22. S.W. Peng, X.Y. Wang, L.S. Dong, Polym. Compos. **26**, 37 (2005)
23. <http://www.rtpcompany.com/PSdata.htm>
24. A.W. Birley, B. Haworth, J. Batchelor, *General Chemical Resistance. Physics of Plastics* (Hanser Publisher, New York, 1992)
25. J.E. Mark, *Polymer Data Handbook* (Oxford University Press, Oxford, 1998)
26. S. Benali, A. Olivier, P. Brocorens, L. Bonnaud, M. Alexandre, S. Bourbigot, E. Espuche, F. Gouanve, R. Lazzaroni, Ph. Dubois, Adv. Mater. Sci. Eng. (2008). doi:10.1155/2008/394235
27. R.B. Seymour, *Engineering Polymer Sourcebook* (McGraw Hill, New York, 1990), pp. 115–117
28. E. Fekete, E. Foldes, F. Damsits, B. Pukanszky, Polym. Bull. **44**, 363 (2000)
29. Qi Yang, Yimin Mao, Guangxian Li, Yajiang Huang, Ping Tang, Mater. Lett. **58**, 3939 (2004)
30. D.R. Paul, C.E. Locke, C.E. Vinson, Polym. Eng. Sci. **13**, 202 (1973)
31. F. Ide, A. Hasegawa, J. Appl. Polym. Sci. **18**, 963 (1974)
32. Jeevanda, T. Siddramaiah, Thermochim. Acta **376**, 51 (2001)
33. R.P. Kambour, J.T. Bendler, R.C. Bopp, Macromolecules **16**, 753 (1983)
34. G. ten Brinke, F.E. Karasz, W.J. MacKnight, Macromolecules **16**, 1827 (1983)
35. D.R. Paul, J.W. Barlow, Polymer **25**, 487 (1984)
36. T. Inoue, T. Soen, T. Hashimoto, H. Kawai, Macromolecules **3**, 87 (1970)
37. S.T. Wellinghoff, J.K. Koenig, E. Baer, J. Polym. Sci. Part B **15**, 1913 (1977)
38. W.C. Lai, W.B. Liau, J. Appl. Polym. Sci. **92**, 1562 (2004)
39. M. Sivakumar, R. Subadevi, S. Rajendran, N.L. Wu, J.Y. Lee, Mater. Chem. Phys. **97**, 330 (2006)
40. D.R. Paul, C.B. Bucknall, *Introduction to Polymer Blends. Formulation*, vol. 1 (Wiley, New York, 2000), pp. 1–14
41. M. De Sarkar, P.P. De, A.K. Bhowmick, Polymer **39**, 6789 (1998)
42. Ming Jiang, Xiu-yun Huang, Yu. Tong-yin, Polymer **24**, 1259 (1983)
43. Jin Kuk Kim Iranian, J. Polym. Sci. Technol. **4**, 210 (1995)
44. M. Hara, J.A. Sauer, J. Macromol. Sci. Rev. Macromol. Chem. Phys. **C38**, 327 (1998)